RESEARCH ARTICLE

Valence energy correction for electron reactive force field

Samuel Bertolini[1] | Timo Jacob[1,2,3]

[1]Institute of Electrochemistry, Ulm University, Ulm, Germany

[2]Helmholtz-Institute Ulm (HIU) Electrochemical Energy Storage, Ulm, Germany

[3]Karlsruhe Institute of Technology (KIT), Karlsruhe, Germany

Correspondence
Samuel Bertolini and Timo Jacob, Institute of Electrochemistry, Ulm University, Albert-Einstein-Allee 47, 89081 Ulm, Germany.
Email: samuel.bertolini@alumni.uni-ulm.de and timo.jacob@uni-ulm.de

Abstract

Reactive force fields (ReaxFF) are a classical method to describe material properties based on a bond-order formalism, that allows bond dissociation and consequently investigations of reactive systems. Semiclassical treatment of electrons was introduced within ReaxFF simulations, better known as electron reactive force fields (eReaxFF), to explicitly treat electrons as spherical Gaussian waves. In the original version of eReaxFF, the electrons and electron–holes can lead to changes in both the bond energy and the Coulomb energy of the system. In the present study, the method was modified to allow an electron to modify the valence energy, therefore, permitting that the electron's presence modifies the three-body interactions, affecting the angle among three atoms. When a reaction path involving electron transfer is more sensitive to the geometric configuration of the molecules, corrections in the angular structure in the presence of electrons become more relevant; in this case, bond dissociation may not be enough to describe a reaction path. Consequently, the application of the extended eReaxFF method developed in this work should provide an improved description of a reaction path. As a first demonstration this semiclassical force field was parametrized for hydrogen and oxygen interactions, including water and water's ions. With the modified methodology both the overall accuracy of the force field but also the description of the angles within the molecules in presence of electrons could be improved.

KEYWORDS
bond cleavage, charge transfer, electrons, eReaxFF, molecular dynamics, water

1 | INTRODUCTION

Computational chemistry is widely used to investigate, on atomistic levels, physical and chemical properties. Quantum mechanical approaches are employed to describe chemical reactions in the fields of batteries, photocatalysis, semiconductor, and so forth.[1–6] On the other hand classical molecular dynamics is often used in biochemistry or to describe fluid properties.[7–9] Additionally, ab initio calculations, due to excessive computational costs, are restricted to small systems and time scales,[10,11] while classical methods can simulate bigger models, but are nonreactive in nature.[12–14]

The ReaxFF[15–18] is a method that is capable to simulate reactions on the fly. Through a bond-order based formalism, the interatomic potential of ReaxFF can even describe reactive events. This allows investigating reaction phenomena (almost) on the same scale as classical force fields.[19] However, ReaxFF operates with electrons implicitly, therefore, the method has limitations to describe systems such as redox reactions in batteries, photocatalysis in fuel cells, or piezo-electric materials. To explicitly treat excess electrons, eReaxFF[20,21] uses spherical Gaussian orbitals[22,23] with constant electron size to describe the electron wave packets, as described by the equation: $\Psi \tilde{e}\text{xp}\left(-\alpha R^2\right)$.

The excess of electrons or electron–holes in eReaxFF is considered as additional particles that carry a charge of -1 or $+1$ e, respectively. But in eReaxFF the excess of electrons does not interact with core or valence electrons of the respective atom. The reason is that the core and valence electrons are treated implicitly by the bond-order approach in ReaxFF. Thus, the electron–electron and electron–nucleus interactions are calculated through the Coulomb point charge and short-range Gaussian wave. Additionally, the number of electrons in a nucleus is determined by an exponential function that decays with distance and can be split between other nuclei. Consequently, the number of excess electrons changes the number of valence electrons of an atom, and therefore the degree of over-coordination of each atom. Because of the modification in the number of valence electrons, the explicit electrons change the under- and over-coordination energy in the ReaxFF routine. However, the corrections for three-body and four-body interactions had not been implemented in the method yet.[20,21]

Force field methods, such as LEWIS[24–26] and electron force fields (eFF),[27,28] include explicit algorithms to describe valence electrons. The capability of both methods to calculate electronic affinities and to handle valence electrons are promising approaches. Nevertheless, the procedures are limited to some range of elements and have not been used to describe complex reactions so far.[29–32] To treat electron–electron and nucleus–electron interactions in eFF, similar to eReaxFF, the methods use Gaussian wave packets to calculate the Coulomb point charge between the particles. However, eFF considered the Gaussian wave packet with a variable size of the electron's wave and includes Pauli repulsion,[32–36] while in eReaxFF electrons have a constant size.

In the eReaxFF method, the energy is calculated for numerous contributions that range from two- to four-body interactions, as well as non-bonded interactions such as van der Waals and Coulomb contributions. The energy contributions can be split into over-coordination penalty, under-coordination stability, lone pair, valence, torsion, and hydrogen bridge energies.[18] The electrostatic interactions can be calculated by the electronegativity equilibration method (EEM)[37,38] when performing standard ReaxFF, however, it includes inadequacies such as long-range charge transfer, noninteger molecular charges at large separations, out-of-plane polarization, and so forth. To impede unphysical long-range charge transfer, the atom-condensed Kohn–Sham (ACKS2)[39] approach provides an extension to the EEM that improves the atom-in-molecu description e.[40] In eReaxFF, the electron and electron–hole can modify only the over-coordination, penalty, under-coordination, and lone pair energy stability, while ACKS2 describes the electrostatic interactions.

This study aimed at modifying the eReaxFF handling of the valence energy, such that an ion can have its angles changing with the presence of electrons. This is motivated by the fact that the presence of excess electrons usually changes the number of lone pairs and sp-orbital hybridizations, consequently modifying the angular structure and possibly entire reaction pathways.[41,42] Thus, we consider that computing the effect on electrons to the valence energy in eReaxFF (controlling the variation in the angular structure due to excess

charges) is important for the accuracy and better prediction of the correct reaction path and structure motifs. The modified approach becomes more relevant when this charge induces changes that are deterministic for the configuration of the system. To achieve this angular structure control, new parameters had to be introduced in the equations. Also, to demonstrate a first application of the new method, a force field was parametrized for H-O interactions. Additionally, the molecular dynamics simulations with water ions appear to agree with the literature.

Restricting the training and validation to hydrogen and oxygen interactions, especially for water, limited the system to small molecules. The advantage of using such a system is the simplification and almost elimination of electron-torsion contributions. Still, our modification in the eReaxFF formalism has the potential to be applicible to even more complex systems that contain more extended molecules and other elements such as carbon, nitrogen, and/or sulfur. Electrolytes for batteries, conductive polymers, and ion transport in organic membranes are examples of fields in which our modification to eReaxFF can be applied as well. Systems in these areas contain complex molecules, where the electron distribution can affect the geometry and overall reactivity. In such systems our method can improve the angle description.

2 | COMPUTATIONAL METHODS

2.1 | Method description

The Software for Chemistry and Materials (SCM, Amsterdam Modeling Suite)[15,16,43] was modified to allow electrons (El) and electron–holes (Eh) corrections for three-body interactions, hence called eReaxFF2, while the original version hereafter will be called eReaxFF. In the new version, eReaxFF2, the valence energy and the angle between each triple of atoms change according to the number of electrons a the central atom j (considering a sequence of three atoms as i–j–k). The equilibrium angle is altered by the valence angle (Val_j^{ang}), the number of lone pairs ($\eta_{lp,j}$), the bond order of atom j (BO_{jn}), and also by the number of El or Eh in the atom j ($n_{el,j}$ or $n_{eh,j}$), as described in Equation (1). A factor (f) that can range between 0 and 1 is added to permit that eReaxFF2 acts as eReaxFF.

$$\Delta_j^{ang} = -Val_j^{ang} + \sum_{i=1}^{neighbors(j)} BO_{ji} - n_{el,j}.f \qquad (1)$$

In a similar equation for the degree of over-coordination for valence electrons (Δ_j^{xel}) in eReaxFF,[20] the degree of over-coordination for valence angle ($\Delta_j^{ang.xel}$) is calculated using the newly introduced parameters (p_{jn}^{xel3} and p_j^{xel4}), according to Equation (2). Thus, the equation depends on the type of bond formed with the central atom, and its bond order between this pair. Additionally, the number of electrons at the central atom and the type of this central atom will affect Equation (2). Through all the equations, Δ_j^{ang} are replaced by $\Delta_j^{ang.xel}$, while the other parts of the equations were not modified (Equations (2)–(4)).

Moreover, the equilibrium angle (θ_0) depends on the sum of p-bond orders (SBO) around the central atom, but the SBO is affected by $\Delta_j^{ang.xel}$ and $\eta_{lp,j}$. Consequently, by modifying SBO, $\Delta_j^{ang.xel}$ and $\eta_{lp,j}$ changes θ_0. Similar as $\Delta_j^{ang.xel}$, the number of lone pairs ($\eta_{lp,j}$) is also modified by the number of excess electrons at the central atom, similarly to Equation (1), and therefore also affects θ_0.

$$\Delta_j^{ang.xel} = \Delta_j^{ang}.\exp\left(p_j^{xel4}.n_{el,j}.\frac{\sum_{i=1}^{neighbors(j)}BO_{ji}.p_{ji}^{xel3}}{\sum_{i=1}^{neighbors(j)}BO_{ji}}\right) \quad (2)$$

$$SBO = \sum_{n=1}^{neighbors(j)}\left(BO_{jn}^{\pi}+BO_{jn}^{\pi\pi}\right)$$
$$+ \left(1 - \prod_{n=1}^{neighbors(j)}\exp\left(BO_{jn}^8\right)\right).\left(-\Delta_j^{ang.xel}-p_{val8}.\eta_{lp,j}\right) \quad (3)$$

$$f_8\left(\Delta_j^{ang.xel}\right) = p_{val5}$$
$$- (p_{val5}-1).\frac{2+\exp\left(p_{val6}.\Delta_j^{ang.xel}\right)}{1+\exp\left(p_{val6}.\Delta_j^{ang.xel}\right)+\exp\left(-p_{val7}.\Delta_j^{ang.xel}\right)} \quad (4)$$

The presence of excess electrons also affects the relevance that the angle will contribute to the valence energy (Equations (5)a and (5) b). The excess of electrons will affect the spring constant of the central atom, linearly proportional to the square difference between the actual and the optimum angle $(\theta_0-\theta_{ijk})^2$. Moreover, the contribution of each bond order to the valence energy (f_7) is also altered by the number of electrons (Equation (6)). Here (f_7), the electron behaves as a pseudo bond order in the valence energy expression. Also, the derivative energy equations were added in the Supporting Information (**Equations S1–S15**) and the code was modified to adapt to the presence of electrons and changes in the derivative energy equations. The energy derivatives are with respect to the bond order, which has no direct physical meaning. The derivatives are also with respect to the distance between electron and nuclei, which gives the interaction forces between electrons and nuclei. The modified equations are activated when a tag in the head file of the force field is set to the force field ([ereaxff2], see Supporting Information), while without the tag, the code performs the original ReaxFF. As can be observed, in many cases, the new derivatives conserve similarities to the original version, for example, f_8' conserves the original equation, and then multiply the equation by $\Delta_j'^{ang.xel}$. This procedure improves the code performance and minimizes the risk to implement a new bug into the code. Comparing the energy gradients, virial equation, and forces, between eReaxFF and eReaxFF2, has some limitations because they represent two different force field parameterizations. Nevertheless, the continuity and similarity of the values (Figure S14) suggest that no additional bugs have been implemented in the code.

The standard ReaxFF formalism contains the parameters p_{val1}, p_{val2}, p_{val3}, p_{val4}, p_{val5}, p_{val6}, and p_{val7}, and θ_0(equilibration angle)[15–18] that determine the functions f_7, f_8, f_9, and f_{val}, and consequently, also the valence energy (E_{val}). The following new parameters were introduced in eReaxFF2:

p_{xel3}, p_{xel4}, p_{xel5}, and p_{xel6}.

$$f_{val}(\theta_0) = p_{val1}.\left(1 - \exp\left(-(p_{val2}+p_{xel5}.n_{el,j}).(\theta_0-\theta_{ijk})^2\right)\right), \text{if } p_{val1} > 0 \quad (5a)$$

$$f_{val}(\theta_0) = p_{val1}.\left(-\exp\left(-(p_{val2}+p_{xel5}.n_{el,j}).(\theta_0-\theta_{ijk})^2\right)\right), \text{if } p_{val1} < 0 \quad (5b)$$

$$f_7\left(BO_{ji}\right) = 1 - \exp\left(-p_{val3}.BO_{ji}^{p_{val4}}\right).\exp\left(-p_{pxel6,j}.n_{el,j}^{p_{val4}}\right) \quad (6)$$

$$E_{val} = f_7\left(BO_{ji}\right).f_7\left(BO_{jk}\right).f_8.f_{val} \quad (7)$$

2.2 | Force field training

We used the covariance matrix adaptation evolution strategy (CMA-ES)[44] to train the force field, operating on the energies obtained through density function theory (DFT) and using the DFT energy values as reference. The different structures and energies were calculated using Gaussian09 (G09)[45] with the M062X hybrid functional and a 6–311++G(p,d) basis set.[46,47] The distinctive structures were optimized and then deformed in the direction of the vibrational modes, having the deformation intensity as a scale vector of the vibration mode vectors (see vibration vector example in Figure S1). The optimized structures were used as a reference to compare the distortion energy; for some reactions, the initial structures were used as reference energies. The force field was parametrized to additionally minimize the differences between the energies obtained by DFT and eReaxFF2 after CMA-ES minimization, such as $e = \sum\left\{\left\|E_i^{DFT}-E_{ref}^{DFT}\right\|\right\} - \left\{\left\|E_i^{eReaxFF2}-E_{ref}^{eReaxFF2}\right\|\right\}$. Here, e is the sum of errors that is minimized, E_i^{method} is a single-point energy and E_{ref}^{method} is the energy of the optimized molecule as a reference structure. Modifying the atoms' positions of an optimized molecule in the direction of the vibrational mode vector, allows scanning through bond dissociation and angle modifications.

The El was centralized in the undercoordinated atoms (e.g., HOO*, * is the location of the El), except for water, where the El is located at the oxygen atom. The Eh were centralized at the atom that is over-coordinated (e.g., H_3O^*, * is the location of the Eh). The energy profile of single-point calculations, comparing to the energies obtained by DFT-M062X and eReaxFF2, as well as the location of the El/Eh, can be seen on the Supporting Information, where the reference structure energy was set to zero (Figures S1–S13). Moreover, we ponder that the force field's training can be further improved for both ReaxFF and eReaxFF2, and the limitation of the method itself can create artifacts in the simulations. But also, we consider that our force field might improve the interactions for H–O atoms. The eReaxFF2 method tends to reduce ~10% or more the sum of errors when compared to the original eReaxFF approach, with a small increment in the computational cost. We excogitate that the force field and methods presented in this study can reasonably simulate ionic

species in water. And as demonstrated in the Supporting Information, eReaxFF2 in the majority of the cases provides improved energy profiles when benchmarked with DFT calculations.

A common approach to train eReaxFF is to parametrize an anion as a new atom (e.g., Ag^+, Li^+), and the El can be added to the nucleus, obtaining the electron affinity of the anion and a neutral atom (e.g., Ag^0, Li^0). This approach uses a quasi-Drude style and does not require explicit training of the Eh, which is a quasiparticle created by the depletion of electrons. This strategy shows good results for monovalent metal atoms.[21,48] Nevertheless, in a system where the same atom can dynamically be in presence of an El or an Eh (e.g., H_3O^+ and OH^-), another procedure may be necessary. Here, the Eh particle is designed to stay as the electron–hole created by a local depletion of electrons, for example, when a H_3O is close enough to an OH. Then the electron moves from H_3O to OH, creating an electron–hole at the H_3O and an excess of an electron at the OH (creating H_3O^+ and OH^-). This strategy has the advantage that the parameters of an already trained ReaxFF can be used, however, generalization tends to lack accuracy for different cases.

In the presence of El, the zero-energy reference is set for the optimized neutral molecule. However, in the presence of an Eh, the parameters were optimized to have the optimized ion as the reference energy. Additionally, the El and Eh interactions were trained, as indicated in Scheme 1. Here, the energy of the isolated neutral molecules was compared with the energy when those molecules were close enough, consequently, the total charge of the system is neutral. However, the charge splits between an anion ($H_5O_2^+$ or H_3O^+) and a cation (OH^-) when the molecules are close enough. Additionally, water is compared with the superposition of El and Eh, and the superposition of two El as compared between OH and OH^{2-}. These procedures

aimed at obtaining electron affinities for negative molecules and to split the charge between different molecules.

Since the calculations involve large-scale distortions in the direction of the vibration vectors and reactions, changes in angles and bond dissociation are well considered in the training set (Figures S1–S13). Additionally, Figure 1 summarizes some of the figures presented in the Supporting Information. Several structures in a neutral system have been calculated, including chemical bond strength for H_2, OH, and O_2; changes in angles and bond dissociations for H_2O, H_3, O_3, HO_2, H_3O, and H_2O_5; proton (H) transfer on the 3 H_2O and 6 H_2O clusters; and changes in torsion, angle, and bond distance for HOOH. The calculations also include generic paths for the reactions: (I) 2 $H_2O = H_3O + OH$; (II) $H_2O + O_2 = HO_2 + OH$; (III) $H_2O = O + H_2$; (IV) $HO_2 = H + O_2$; (V) $H_2O = HO + H$; and (VI) $H_2 + O_2 = H_2O + O$; (VII) $O_3 = O_2 + O$. In a charged system containing one El, the electron affinity is calculated by setting the neutral molecule as reference, then distortion is applied to the molecules, allowing changes in angles and bond dissociations. For the systems containing El, we considered (* indicates that the El/Eh is located on the center of the left atom): HH^{*-1}, HO^{*-1}, OO^{*-1}, H_2O^*, HHH^{*-1}, a cluster of $5 \cdot H_2O \cdot HO^{*-1}$, HOO^{*-1}, and OOO^{*-1}. In the presence of an Eh, the optimized charge is the reference and compared with the distorted molecule and, therefore, we calculated H_3O^{*+1} and $H_5O_2^{*+1}$ ($H_2O\text{-}H^*\text{-}OH_2^{+1}$).

2.3 | Molecular dynamics cells

All the molecular dynamics simulations were performed for 20 ps with a step size of 0.25 fs, in a canonical ensemble (NVT), and with the
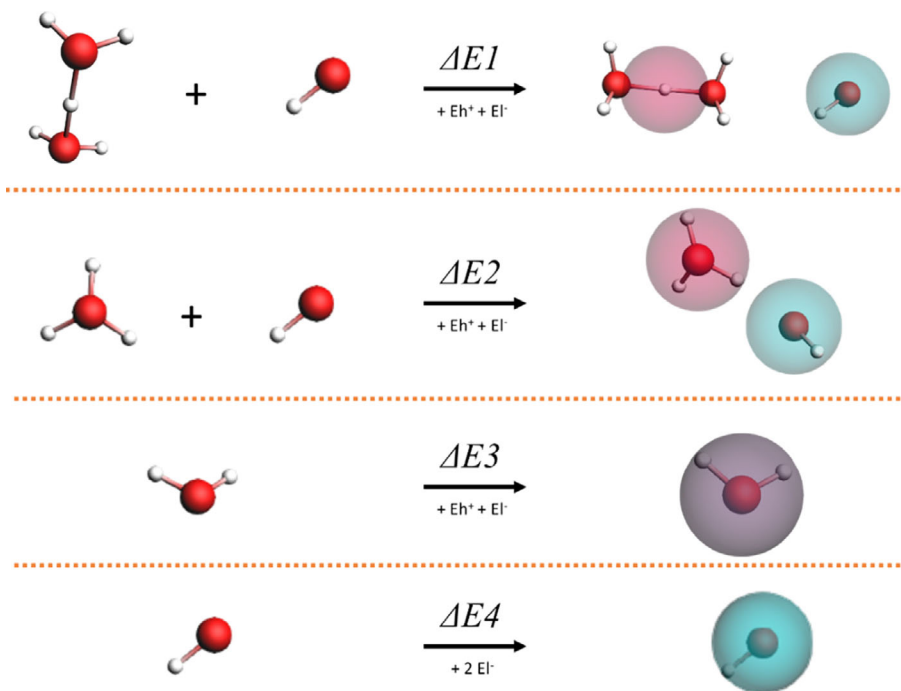
SCHEME 1 This scheme was used to calculate electrons (El) and electron–hole (Eh) interactions. Calculations of El and Eh were done by comparing isolated neutral molecules (H_3O, H_5O_2, and OH) with the close molecules, thus when the charge is split into two ionic species in an overall neutral system (H_3O^+, $H_5O_2^+$, and OH^-). Additionally, annihilation by El and Eh by their superposition was compared with a neutral molecule (H_2O). The superposition of El in OH^{2-} was compared with the neutral molecule (OH)
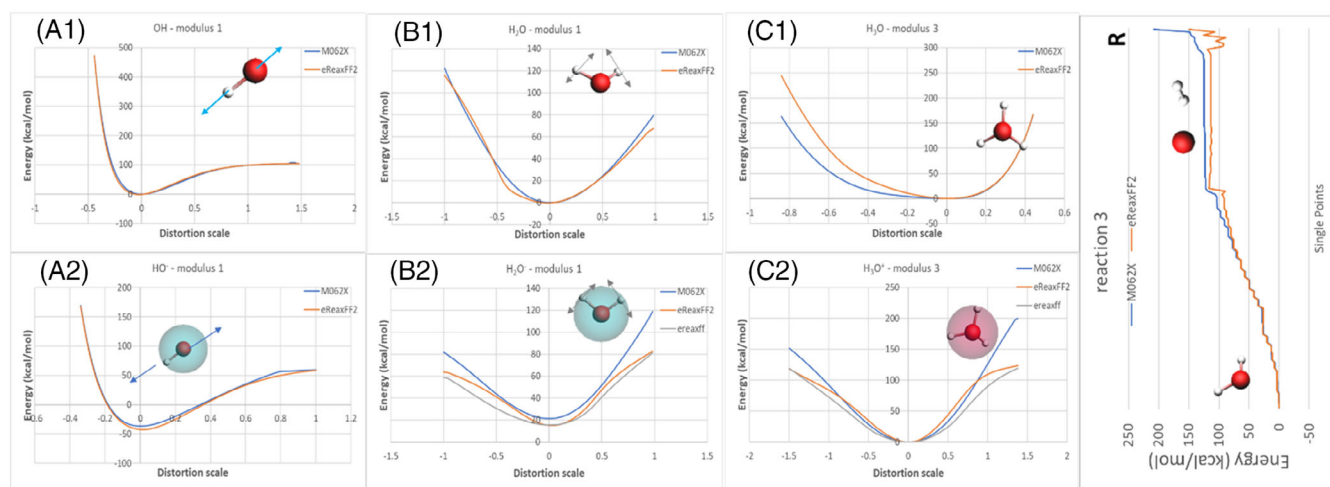
FIGURE 1 Single point calculations comparing DFT-M062X (blue), eReaxFF and the eReaxFF2 (orange) methods. The molecules are distorted in the directions of the vibrational modes, and the distortion allows scanning the energy profile considering bond dissociation and angle changes. The following molecules were trained: A.1) OH; A.2) OH$^-$; B.1) H_2O; B.2) H_2O^-; C.1) H_3O; C.2) H_3O+; and R) the reaction $H_2O = O + H_2$

TABLE 2 Amount of molecules set in the unit cells for the molecular dynamics simulation, in neutral systems and ionic systems.

Name	Molecules				
	H_2O	H_3O	OH	H_3O^+	OH$^-$
a–b	105	15	0	0	0
c–d	132	0	5	0	0
e–f	103	5	5	0	0
g–h	105	0	0	15	0
i–j	109	0	0	0	5
k–l	112	0	0	1	1

Note: The names link to Figure 2.

temperature set to 298 or 1800 K. The cells were divided into two groups: neutral systems and ionic systems, where the ReaxFF and eReaxFF2 methods were investigated respectively. The cells were cubic boxes with a lattice parameter of 15 Å. The density of the cells was ~1.0 g/cm^3, and the amount of molecules in each cell is shown in Table 2.

3 | RESULTS AND DISCUSSION

3.1 | General concepts

Both eReaxFF and eReaxFF2 treat the excess of El or Eh without interacting with the core and valence electrons, and with spherical symmetry. Nevertheless, errors can be minimized by parametrizing β and α parameters, while computation efficiency is maximized by treating only excess El and Eh. Furthermore, the energy due to electron/valence-electron interactions is implicitly present when the electron changes the degree of bond order. Calculating the El/Eh with a

constant electron size (α) can cause errors in the calculation, however, as long as the El/Eh is close to a nucleus, using α in order to set the electron size in an atom is a reasonable approximation. This allows the El to alter its size according to the nucleus. Although eReaxFF and eReaxFF2 have limitations and there is room for future implementations, both methods have the potential to well-describe systems containing ions. The El/Eh localization will also affect the results (here the El/Eh was located in the center of the nuclei), however, a better procedure would be to set the El/Eh between the nuclei.

The eReaxFF2 method allows El to modify the equilibrium angle in three-body interactions, thus, correcting the angles of an ion. The equilibrium angle is modified by $\Delta_j^{ang.xel}$ and $\eta_{lp,j}$. When the system is out of the equilibrium angle, the strength to assume equilibrium is dependent on the angle difference ($\theta_0 - \theta_{ijk}$). The El acts as a spring multiplier factor for the angle difference, reducing or increasing the strength constant of the spring (f_{val}). Therefore, the valence energy goes to zero when the system finds its equilibrium angle. Moreover, the valence energy is also altered by the bond order of the atoms around the central atom (f_7). Because El behaves as a pseudo bond order in $\Delta_j^{ang.xel}$, Δ_j^{xel}, and $\eta_{lp,j}$, the electron can also affect the valence energy as a pseudo bond order (f_7).

The quality of eReaxFF2 to describe ions will very much depend on the quality of ReaxFF to describe a neutral system. When electrons are absent in a nucleus, this nucleus behaves as described in ReaxFF. Moreover, the electron affinity of each ion is calculated through the eReaxFF method. Since eReaxFF is incorporated inside eReaxFF2, the ability of eReaxFF2 to calculate electron affinities depends on the bond energy calculations performed by eReaxFF.

In a DFT simulation, the electrons are distributed in agreement with the nuclei positions. In eReaxFF2, although the mobility of the electrons can be controlled by the electron's mass (here set to be 1 a.u.), tunneling effects are not able to occur because of the particle description of El and Eh performed by eReaxFF. Nevertheless, eReaxFF2

allows localizing the electrons, which allows simulating, for example, electron beam irradiation, ion diffusion in electrolytes, or the reduction of ions at metals. Additionally, eReaxFF2 permits simulating bigger models compared to DFT, thus, being a promising method when ions are part of the system. Considering the CPU time (user + system) of 62,825.65 s to run the molecular dynamic of H_2O and H_3O+ (Figure 2B) using eReaxFF; to run the same simulation with eReaxFF2, the CPU time increased 0.68%, which can be considered a small increment in the computational cost. The eReaxFF2 approach will come with approximately the same pros and cons as the standard ReaxFF or eReaxFF approaches. Comparing these methods, eReaxFF2 has the advantage to improve the reaction path energy profile in presence of El or Eh. As aforementioned, eReaxFF2 can reduce at least 10% of accumulated error of the training when compared to eReaxFF. Nevertheless, because the valence energy is altered by the presence of electrons, also the force between El or Eh with an atom (due to $\partial E_{val}/\partial r$) is affected in the eReaxFF2 method, therefore repulsive force can casue the El/Eh to escape from the nucleus.

3.2 | Single point calculations

The forces that apply to each atom are calculated by the derivative energy equations (Equations S1–S15). Nevertheless, the forces applied to each atom of H_2O^{1-}, where the distortion modulus modifies the water molecule's angle (Figure S14), indicate that eReaxFF2 leas to a similar slope as eReaxFF, despite the apparent differences between both methods. The continuity of the energy gradient suggests that no new bugs were introduced in the code.

The energy profile calculated with the eReaxFF2 method shows similar values when compared with DFT-M062X, especially when the molecules were neutral and the eReaxFF2 behaves like a common ReaxFF, where in the majority of the calculations the methods overlap each other. Nevertheless, some of the results can deviate at strong deformation, for example at high temperatures (Figures S1–S7). The bond energy interaction will determine the electron affinity of a molecule, shifting the molecule energy according to the presence of an electron. eReaxFF2 will accommodate the changes that electrons
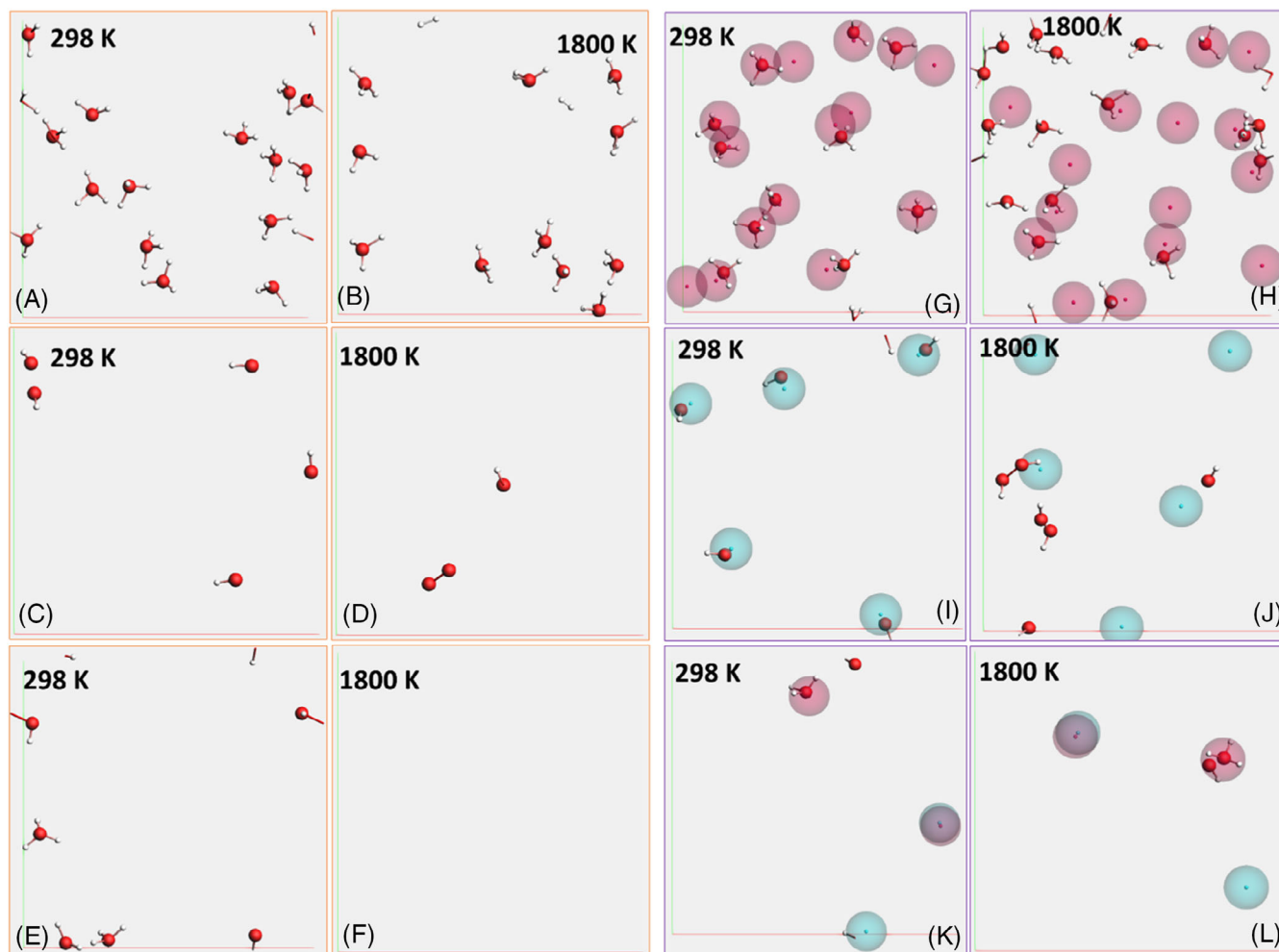
FIGURE 2 Molecular dynamics simulations after 20 ps, where water is hidden from visualization. The systems were initially composed of: (A) H_2O and H_3O at 298 K; (B) H_2O and H_3O at 1800 K; (C) H_2O and OH at 298 K; (D) H_2O and OH at 1800 K; (E) H_2O, H_3O, and OH at 298 K; (F) H_2O, H_3O, and OH at 1800 K; (G) H_2O and H_3O^+ at 298 K; (H) H_2O and H_3O^+ at 1800 K; (I) H_2O and OH^- at 298 K; (J) H_2O and OH^- at 1800 K; (K) H_2O, H_3O^+, and OH^- at 298 K; and (L) H_2O, H_3O^+, and OH^- at 1800 K

TABLE 1 Energetics of electron and electron hole affinity as described in Scheme 1.

kcal/mol	ΔE_1	ΔE_2	ΔE_3	ΔE_4
DFT	−12.91	−66.19	0.00	−95.11
eReaxFF2	−62.18	−66.31	0.08	−95.12

apply to the three-body interactions, consequently, the quality eReaxFF2 is correlated with the aptitude of eReaxFF to describe electron affinities. In general, eReaxFF2 can reasonably well calculate ionic molecules (Figures S8–S13). Moreover, comparing the results obtained by DFT-M062X and eReaxFF2, the interactions involving El and Eh on the same system, as described in Scheme 1, are comparable. The values shown in Scheme 1 and summarized in Table 1 are (DFT-M062X/eReaxFF2): $\Delta E_1 = -12.91/-62.18$ kcal/mol, $\Delta E_2 = -66.19/-66.31$, $\Delta E_3 = 0.00/0.08$ kcal/mol, and $\Delta E_4 = -95.11/-95.12$, respectively. When the El or Eh is centralized at a hydrogen atom, our force field fails to accurately describe the electron affinity of a molecule, for example, the discrepancy between DFT-M062X and eReaFF2 for ΔE_1, or distortion when compared to the energy profiles for $H_2O_5^+$. Nevertheless, when the El or Eh is located at an oxygen atom, our force field can describe electron affinity with higher accuracy.

3.3 | Molecular dynamics simulations

First, comparing the temperature effect in the molecular dynamics simulation (Figure 2, at 20 ps), the temperature will have two effects on the simulation: one is to accelerate the occurrence of reactions, and another is to see that the El/Eh escapes from one nucleus to another.

When H_2O and H_3O were present in the system, at 298 K, no reactions were observed during the simulation, however, at 1800 K, H_3O reacted and produced H_2 and H_2O (Figures 2A,B). When H_3O^+ was present in the system, H_3O^+ can form H_4O^+ and H_2O, releasing one Eh to the system (Figure 2G). Although tetravalent oxygen can exist in superacids,[49,50] the formation of H_4O^+ may be an artifact of the simulation. Because only one H_4O^+ is formed in the presence of 15 H_3O^+, the reaction tends to be concentration-dependent, and the formation of H_4O^+ was not observed at low concentrations (Figure 2K,L), supporting this assumption. The same does not happen at 1800 K, where H_3O^+ does not react, but Eh can be removed and reabsorbed by H_3O^+ (Figure 2G).

In the presence of H_2O and OH (Figure 2C,D), when HOOH is formed, HOOH becomes stable in the media. At 298 K, the formation of HOOH was not observed, which can be due to the diffusion process and temporary reactions between H_2O and OH. While at 1800 K, HOOH was formed and also reacted, forming O_2 and H_2O. In the presence of H_2O and OH⁻ (Figure 2I,J), HOOH⁻ is not stable, it can be formed more often at 1800 K than 298 K, but the El breaks the molecules, forming again OH and OH⁻.

When the system contains H_2O, H_3O, and OH (Figure 2E,F), the reaction between H_3O and OH produces H_2O, and the temperature has only the effect to accelerate the reactions, and also at 298 K hydrogen peroxide (HOOH) is formed during the reactions. When H_2O, H_3O^+, and OH⁻ were in the same cell, no formation of water could be observed neiter at lower nor at higher temperatures (Figure 2K,L), and the El and Eh set initially in the water molecule stays overlapping the oxygen atom of H_2O.

3.4 | Comparison with experiments

The results observed in the molecular dynamics simulations are consistent with experimental and theoretical investigations. Although our trained force field appears to well mimic the energy profile of proton transfer in water at low and high distortions, a systematic investigation of water structure, density, and reaction kinetics should take place. Nevertheless, our simulations could reproduce results from other investigations: the formation of tetravalent oxygen (H_4O^+) in superacids[49,50]; the decomposition of hydrogen peroxide (HOOH) by hydroxide (OH) attack to form water (H_2O) and oxygen gas (O_2)[51]; the production of HOOH by OH reaction,[52] the formation of H_3O_2 as proton transfer between H_2O and OH[53]; the predominance of Eigen[54] ions over Zundel[55] ions (starting with predominant Eigen ions),[56] and the formation of H_2 only from two H_3O molecules. But the deprotonation of H_3O in water[57] was not observed. Comparison with further experimental results is not trivial because of the limitation to reproducing the presence of a high concentration of water ions (H_3O^+ and OH⁻) without the presence of a countger-ion (e.g., Na⁺) or catalyst material. Still, eReaxFF2 allows one to isolate a target ion to analyze, for example, diffusion processes. The stability of H_3O^+ and OH⁻ suggests that eReaxFF can simulate systems containing ions. When the intention is to simulate ions such as H_3O^+ or OH⁻, instead of H_3O or OH, the presence of El or Eh eliminate the risk of unexpected reactions that can exist in ReaxFF (e.g., formation of H_2 during a collision of H_3O^+).

4 | CONCLUSIONS

In this work, we have modified the standard eReaxFF by modifying the three-body interaction, here called eReaxFF2. Then the new parameters and the parameters of standard ReaxFF and eReaxFF have been trained for hydrogen and oxygen interactions (benchmarking with DFT-MP02X). The eReaxFF2 methods can adapt the angles of the molecule in presence of El and Eh, and can also give the electron affinity of molecules. However, the eReaxFF2 method still has limitations: 1) it does not correct the torsion energy in presence of electrons; 2) the excess electrons do not interact with the core and valence electrons of an atom; 3) the electron has a constant size and cannot reproduce excitations; 4) the electron cannot tunnel; 5) the excess electron behaves only as spherically symmetric with a homogeneous distribution. Consequently, the method can fail to well-describe

certain reactions, and therefore the eReaxFF2 method should be compared with DFT or another more accurate method for validation. The same applies to ReaxFF, which also should be benchmarked against more accurate methods. Nevertheless, eReaxFF2 can handle larger scale systems over longer time periods. Additionally, with our test system we could show that eReaxFF2 can simulate ions in water, in agreement with experimental observations.

For the systems that contain H–O interactions, the system can satisfactorily describe neutral and ionic molecules. The molecular dynamics show that increasing the temperature also leads to an increase in reactivity and helps removing the excess of El and Eh from the nuclei. The molecular dynamics also suggest that El and Eh can stabilize ionic molecules. Thus, we consider that eReaxFF2 can also be used as a semiclassical force field for the investigation of water splitting. As mentioned above, eReaxFF2 can reduce the sum of errors, benchmarking with DFT calculations, by ~10% or more, at a low computational cost. In conclusion, eReaxFF2 does improve the predictions of verifiable results from condensed-phase molecular dynamic simulations, including water.

ACKNOWLEDGMENT

CONFLICT OF INTEREST

There are no conflicts to declare.

DATA AVAILABILITY STATEMENT

Data available on request from the authors, and code data subject to third party restrictions.

ORCID

Samuel Bertolini 🔟 https://orcid.org/0000-0003-0969-7142
Timo Jacob 🔟 https://orcid.org/0000-0001-7777-2306

REFERENCES

[1] L. E. Camacho-Forero, T. W. Smith, S. Bertolini, P. B. Balbuena, *J Phys Chem C* **2015**, *119*, 26828.

[2] S. Bertolini, P. B. Balbuena, *Electrochim Acta* **2017**, *258*, 1320.

[3] D. Rodney, L. Ventelon, E. Clouet, L. Pizzagalli, F. Willaime, *Acta Mater* **2017**, *124*, 633.

[4] S. Bertolini, T. Jacob, *Electrochem Sci Adv*, **2021**, *403*, e2100088.

[5] S. Bertolini, T. Jacob, *ACS Omega* **2021**, *6*, 9700.

[6] S. Bertolini, T. Jacob, *J Energy Chem* **2022**, *66*, 587.

[7] S. H. Jamali, L. Wolff, T. M. Becker, M. T. de Groen, M. Ramdin, R. Hartkamp, A. Bardow, T. J. Vlugt, O. A. Moultos, *J Chem Inf Model* **2019**, *59*, 1290.

[8] H. C. Thielemann, A. Cardellini, M. Fasano, L. Bergamasco, M. Alberghini, G. Ciorra, E. Chiavazzo, P. Asinari, *J Mol Model* **2019**, *25*, 147.

[9] H. Ye, Z. Shen, Y. Li, *Comput Mech* **2018**, *62*, 457.

[10] O. Prezhdo, *Astrophys Data Syst* **2017**, *K7*, 004.

[11] Z. Liu, S. Bertolini, P. B. Balbuena, P. P. Mukherjee, *ACS Appl Mater Interfaces* **2016**, *8*, 4700.

[12] H. Sun, Z. Jin, C. Yang, R. L. Akkermans, S. H. Robertson, N. A. Spenley, S. Miller, S. M. Todd, *J Mol Model* **2016**, *22*, 47.

[13] J. Huang, A. D. MacKerell Jr.., *J Comput Chem* **2013**, *34*, 2135.

[14] K. Lindorff-Larsen, S. Piana, K. Palmo, P. Maragakis, J. L. Klepeis, R. O. Dror, D. E. Shaw, *Proteins* **2010**, *78*, 1950.

[15] A. C. Van Duin, S. Dasgupta, F. Lorant, W. A. Goddard, *Chem A Eur J* **2001**, *105*, 9396.

[16] K. Chenoweth, A. C. Van Duin, W. A. Goddard, *Chem A Eur J* **2008**, *112*, 1040.

[17] S. J. Stuart, A. B. Tutein, J. A. Harrison, *J Chem Phys* **2000**, *112*, 6472.

[18] T. P. Senftle, S. Hong, M. M. Islam, S. B. Kylasa, Y. Zheng, Y. K. Shin, C. Junkermeier, R. Engel-Herbert, M. J. Janik, H. M. Aktulga, *NPJ Comput Mater* **2016**, *2*, 1.

[19] S. Bertolini, P. B. Balbuena, *J Phys Chem C* **2018**, *122*, 10783.

[20] M. M. Islam, G. Kolesov, T. Verstraelen, E. Kaxiras, A. C. Van Duin, *J Chem Theory Comput* **2016**, *12*, 3463.

[21] M. M. Islam, A. C. Van Duin, *J Phys Chem C* **2016**, *120*, 27128.

[22] A. A. Frost, *J Chem Phys* **1967**, *47*, 3707.

[23] A. A. Frost, *J Chem Phys* **1967**, *47*, 3714.

[24] S. Kale, J. Herzfeld, S. Dai, M. Blank, *J Biol Phys* **2012**, *38*, 49.

[25] S. Kale, J. Herzfeld, *J Chem Theory Comput* **2011**, *7*, 3620.

[26] S. Kale, J. Herzfeld, *J Chem Phys* **2012**, *136*, 084109.

[27] J. T. Su, W. A. Goddard III., *J Chem Phys* **2009**, *131*, 244501.

[28] J. T. Su, W. A. Goddard III., *Phys Rev Lett* **2007**, *99*, 185003.

[29] S. Ekesan, J. Herzfeld, *Proc Royal Soc A: Math Phys Eng Sci* **2015**, *471*, 20150370.

[30] S. Ekesan, S. Kale, J. Herzfeld, *J Comput Chem* **2014**, *35*, 1159.

[31] S. Kale, *Reactive Force Fields via Explicit Valency*, Brandeis University, Waltham, MA **2012**.

[32] A. Jaramillo-Botero, J. Su, A. Qi, W. A. Goddard III., *J Comput Chem* **2011**, *32*, 497.

[33] D. Klakow, P.-G. Reinhard, C. Toepffer, *Ann Phys* **1997**, *259*, 141.

[34] B. Jakob, P.-G. Reinhard, C. Toepffer, G. Zwicknagel, *Phys Rev E* **2007**, *76*, 036406.

[35] D. Klakow, C. Toepffer, P. G. Reinhard, *J Chem Phys* **1994**, *101*, 10766.

[36] M. Knaup, P. Reinhard, C. Toepffer, G. Zwicknagel, *J Phys A Math Gen* **2003**, *36*, 6165.

[37] W. J. Mortier, S. K. Ghosh, S. Shankar, *J Am Chem Soc* **1986**, *108*, 4315.

[38] P. Bultinck, W. Langenaeker, P. Lahorte, F. De Proft, P. Geerlings, M. Waroquier, J. Tollenaere, *Chem A Eur J* **2002**, *106*, 7887.

[39] T. Verstraelen, P. Ayers, V. Van Speybroeck, M. Waroquier, *J Chem Phys* **2013**, *138*, 074108.

[40] I. Leven, H. Hao, S. Tan, X. Guan, K. A. Penrod, D. Akbarian, B. Evangelisti, M. J. Hossain, M. M. Islam, J. P. Koski, *J Chem Theory Comput* **2021**, *17*, 3237.

[41] J. J. Butler, T. Baer, S. A. Evans Jr.., *J Am Chem Soc* **1983**, *105*, 3451.

[42] E. Miliutina, O. Guselnikova, N. S. Soldatova, P. Bainova, R. Elashnikov, P. E. Fitl, T. Kurten, M. S. Yusubov, V. C. Švorčík, R. R. Valiev, *J Phys Chem Lett* **2020**, *11*, 5770.

[43] C. Dulong, B. Madebene, S. Monti, J. Richardi, *J Chem Theory Comput* **2020**, *16*(11), 7089.

[44] M. W. Iruthayarajan, S. Baskar, *Expert Syst Appl* **2010**, *37*, 5775.

[45] M. J. Frisch, G. W. Trucks, H. B. Schlegel, G. E. Scuseria, M. A. Robb, J. R. Cheeseman, G. Scalmani, V. Barone, B. Mennucci, G. A. Petersson, H. Nakatsuji, M. Caricato, X. Li, H. P. Hratchian, A. F. Izmaylov, J. Bloino, G. Zheng, J. L. Sonnenberg, M. Hada, M. Ehara, K. Toyota, R. Fukuda, J. Hasegawa, M. Ishida, T. Nakajima, Y. Honda, O. Kitao, H. Nakai, T. Vreven, J. A. Montgomery Jr., J. E. Peralta, F. O. Ogliaro, M. J. Bearpark, J. Heyd, E. N. Brothers, K. N. Kudin, V. N.

Staroverov, R. Kobayashi, J. Normand, K. Raghavachari, A. P. Rendell, J. C. Burant, S. S. Iyengar, J. Tomasi, M. Cossi, N. Rega, N. J. Millam, M. Klene, J. E. Knox, J. B. Cross, V. Bakken, C. Adamo, J. Jaramillo, R. Gomperts, R. E. Stratmann, O. Yazyev, A. J. Austin, R. Cammi, C. Pomelli, J. W. Ochterski, R. L. Martin, K. Morokuma, V. G. Zakrzewski, G. A. Voth, P. Salvador, J. J. Dannenberg, S. Dapprich, A. D. Daniels, Ã. D. N. Farkas, J. B. Foresman, J. V. Ortiz, J. Cioslowski, D. J. Fox, *Gaussian 09*, Gaussian, Inc., Wallingford, CT, USA **2009**.

[46] A. D. Becke, *J Chem Phys* **1993**, *98*, 5648.

[47] J. P. Perdew, J. A. Chevary, S. H. Vosko, K. A. Jackson, M. R. Pederson, D. J. Singh, C. Fiolhais, *Phys Rev B* **1992**, *46*, 6671.

[48] B. Evangelisti, K. A. Fichthorn, A. C. Van Duin, *J Chem Phys* **2020**, *153*, 104106.

[49] S. J. Grabowski, D. Casanova, E. Formoso, J. M. Ugalde, *ChemPhysChem* **2019**, *20*, 2443.

[50] G. A. Olah, G. S. Prakash, M. Barzaghi, K. Lammertsma, P. V. R. Schleyer, J. A. Pople, Protonated hydronium dication, H_4O^{2+}: hydrogen–deuterium exchange of $D_2H_{17}O^+$ in HF: SbF_5 and $DH_{217}O^+$ in DF: SbF_5 and theoretical calculations. in *Across Conventional Lines: Selected Papers of George A Olah*, Vol. 2, World Scientific, Los Angeles, CA **2003**, p. 837.

[51] R. J. Watts, M. K. Foget, S.-H. Kong, A. L. Teel, *J Hazard Mater* **1999**, *69*, 229.

[52] L. Brouwer, C. Cobos, J. Troe, H. R. Dübal, F. Crim, *J Chem Phys* **1987**, *86*, 6171.

[53] J. Andres, M. Duran, A. Lledos, J. Bertran, *Chem Phys Lett* **1986**, *124*, 177.

[54] M. Eigen, *Angew Chem Int Ed* **1964**, *3*, 1.

[55] G. Zundel, H. Metzger, *Z Phys Chem* **1968**, *58*, 225.

[56] A. Botti, F. Bruni, M. Ricci, A. Soper, *J Chem Phys* **2006**, *125*, 014508.

[57] D. Talbi, R. P. Saxon, *J Chem Phys* **1989**, *91*, 2376.

SUPPORTING INFORMATION

Additional supporting information may be found in the online version of the article at the publisher's website.